Volume 1 | Number 1 | Jan 2013 | Pages 1–100

Dalton Transactions

An international journal of inorganic chemistry
www.rsc.org/dalton

ROYAL SOCIETY OF CHEMISTRY

ROYAL SOCIETY OF CHEMISTRY

www.rsc.org/dalton

Journal Name

Dynamic Article Links ▶

ARTICLE TYPE

Synthesis, Structure and Properties of [Co(NCS)₂(4-(4-Chlorobenzyl) pyridine)₂]ₙ, that shows Slow Magnetic Relaxations and a Metamagnetic Transition

Julia Werner[a], Zbigniew Tomkowicz[b], Michał Rams[b], Stefan G. Ebbinghaus[c], Tristan Neumann[a] and Christian Näther*[a]

Reaction of Co(NCS)₂ with 4-(4-chlorobenzyl)pyridine (ClBP) leads to the formation of Co(NCS)₂(4-(4-chlorobenzyl)pyridine)₄ (**1**) and [Co(NCS)₂(4-(4-chlorobenzyl)pyridine)₂]ₙ (**2**). In the crystal structure of **1** the Co(II) cations are octahedrally coordinated by two terminal bonded thiocyanato anions and four ClBP ligands, whereas in **2** the Co(II) cations are linked into chains by pairs of μ-1,3-bridging thiocyanato anions. Magnetic measurements on **2** show an antiferromagnetic phase transition with T_N = 3.9 K. A metamagnetic transition is observed at the critical magnetic field of 260 Oe. Magnetic relaxations in zero field are consistent with single chain magnetic behavior. These results are compared with those obtained for similar compounds reported recently.

Introduction

Low-dimensional magnetic materials because of their unusual properties attracted wide interest of researches through several decades. The last wave of interest is related with the discovery of the so called Single Chain Magnets (SCM) and an increasing number of such compounds are continuously reported.[1-9] In this regard compounds that show a slow relaxation of the magnetization that can be traced back to the relaxation of single chains are of special interest because of their potential for future applications as high-density storage material.[10-27] To get more insight into the influence of a chemical and a structural modification onto the magnetic properties of such compounds systematic investigations using strongly related compounds are needed.

For the creation of such materials, it is necessary that cations of large magnetic anisotropy are linked into chains by small ligands like, e.g. azido anions that can mediate strong magnetic exchange along the chains.[28-31] In this context thiocyanato ligands are also useful because they offer a broad number of different bonding modes, which allows the selective preparation of coordination compounds with a different dimensionality of the coordination network.[32-53]

In our ongoing project on the synthesis, structure and properties of thio- or selenocyanato coordination polymers we are especially interested in compounds, in which Co(II) or Fe(II) cations are connected by pairs of these anionic ligands into chains, because several of them show a slow relaxation of the magnetization, indicative for SCM behavior. For the first time we observed such relaxations in [Co(NCS)₂(pyridine)₂]ₙ,.[54] A similar behavior is observed for the corresponding selenocyanato coordination polymer [Co(NCSe)₂(pyridine)₂]ₙ, with significantly stronger intrachain interactions.[55] In contrast, the analogous Fe(II) compound [Fe(NCS)₂(pyridine)₂]ₙ reported by Foner *et al*. is a metamagnet that shows no relaxations but this behavior can be induced by exchange of the anionic ligand.[56-57] [Fe(NCSe)₂(pyridine)₂]ₙ is also a metamagnet but it shows slow relaxation of the magnetization and it is assumed that the lower magnetic anisotropy of Fe(II) cations is compensated by stronger intrachain interactions.[58]

To study the influence of the co-ligand onto the relaxation properties, compounds with different co-ligands were prepared that also consist of 1D Co(NCS)₂ chains and also show these relaxations. This includes, e.g., [Co(NCS)₂(4-acetylpyridine)₂]ₙ that exhibit a ferromagnetic ground state.[59] In contrast, [Co(NCS)₂(4-ethylpyridine)₂]ₙ, has an antiferromagnetic ground state and shows a metamagnetic transition.[60] A similar behavior is also observed for [Co(NCS)₂(bis-(4-pyridyl)ethylene)₂]ₙ and for [Co(NCS)₂(bis-(4-pyridyl)ethane)₂]ₙ.[39, 61] We also tried to investigate the influence of the interchain interactions by using the relatively large 4-(3-phenylpropyl)pyridine as co-ligand. [Co(NCS)₂(4-(3-phenylpropyl)pyridine)₂]ₙ exhibits a ferromagnetic ground state and also shows magnetic relaxations that, however, cannot be clearly attributed to single chain relaxations.[62]

To investigate the influence of the co-ligand onto the magnetic properties in more detail we tried to prepare a compound based

on the relatively large co-ligand 4-(4-chlorobenzyl)pyridine, in which the Co cations are linked by pairs of μ-1,3-bridging thiocyanato anions into chains. Here we report on our investigations.

Results and Discussions

Synthesis and Crystal structures

Reaction of different ratios of $Co(NCS)_2$ and 4-(4-chlorobenzyl)pyridine leads to the formation of two different compounds as indicated by X-ray powder diffraction. The results of the elemental analysis reveal a composition of $Co(NCS)_2(ClBP)_4$ (**1**) and of $Co(NCS)_2(ClBP)_2$ (**2**). In compound **1** the asymmetric stretching vibration $\nu_{as}(CN)$ is observed at 2064 cm^{-1}, which proves that only N-terminally bonded thiocyanato anions are present. In contrast, in compound **2** the asymmetric stretching vibration $\nu_{as}(CN)$ is shifted to 2105 cm^{-1}, which indicates that μ-1,3 bridging thiocyanato anions are present (Figure S1 and S2 in the Supporting Information). Based on these results it can be concluded that compound **1** consists of octahedrally coordinated discrete complexes, whereas in compound **2** the cations are linked by the anionic ligands into a coordination polymer. To verify if compound **1** could be used as a precursor to prepare a ligand deficient phase by thermal decomposition, measurements using simultaneous differential thermoanalysis and thermogravimetry were performed. This shows that compound **1** decompose in only one step at about 120°C, without the formation of any further intermediate (Figure S3 in the Supporting Information). Single crystals were obtained from acetonitrile (**1**) or methanol (**2**) and were characterized by single crystal x-ray diffraction.

$Co(NCS)_2(ClBP)_4$ (**1**) crystallizes in the monoclinic space group *C*2/c with four formula units in the unit cell. The asymmetric unit consists of one cobalt cation which is located on a center of inversion as well as of one thiocyanato anion and two 4-(4-chlorobenzyl)pyridine ligands in general position. The metal center is octahedrally surrounded by two thiocyanato anions and four 4-(4-chlorobenzyl)pyridine ligands (Figure 1).
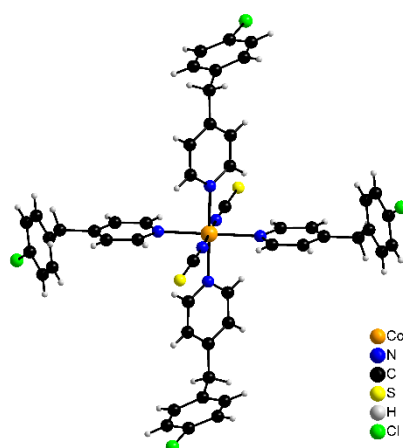

Figure 1. Coordination sphere of **1**. An ORTEP plot of this structure can be found in Figure S4 in the Supporting Information.

The cobalt nitrogen distances range between 2.0943(15) and 2.241(2) Å and the bond angles have values between 88.66(6) and 91.34(6)° and of 180.00(8)° (Table S1 in the Supporting Information).

$[Co(NCS)_2(ClBP)_2]_n$ (**2**) crystallizes in the triclinic space group *P*-1 with two formula units in the unit cell. The asymmetric unit consists of two crystallographically independent cobalt cations

which are located on centers of inversion as well as of two thiocyanato anions and two 4-(4-chlorobenzyl)pyridine ligands in general positions. The cobalt cations are in an octahedral environment and are coordinated by two ClBP ligands and by two N and two S atoms of four thiocyanato anions in *trans* position (Figure 2). The cobalt nitrogen distances range from 2.060(2) to 2.165(2) Å and the Co-S distances are between 2569(1) and 2.607(1) Å (Table S2 in the Supporting Information). The overall coordination of both crystallographically independent Co cations is almost identical.
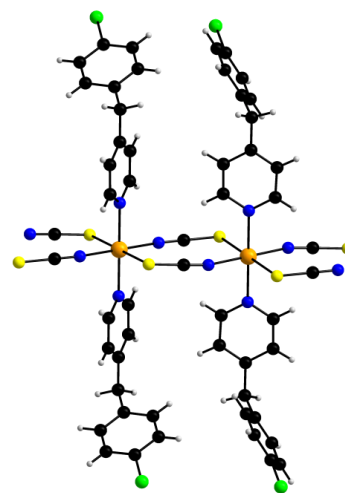
Figure 2. View of the coordination sphere of **2**. An ORTEP plot of **2** can be found in Figure S5 in the Supporting Information.

The Co cations are linked by pairs of μ-1,3-bridging thiocyanato anions into chains with an interchain distance of 5.6348 Å between neighboring Co cations (Figure 2). The shortest interchain Co···Co distance amounts to 8.2413 Å. In the crystal structure the cobalt thiocyanato chains are oriented parallel to each other and this arrangement is similar to that in $[Co(NCS)_2(pyridine)_2]_n$ and $[Co(NCS)_2(4\text{-}Acpy)_2]_n$ reported recently.[54]
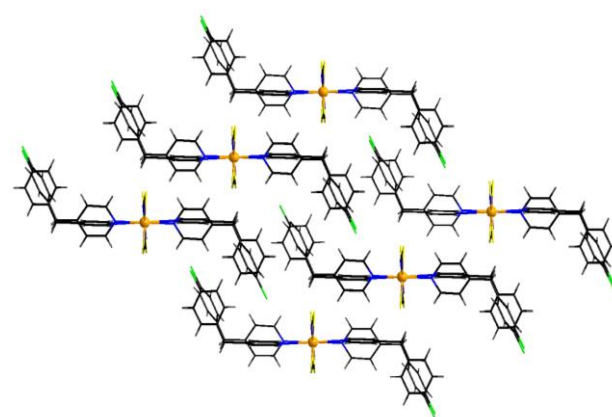
Figure 3. View of the arrangement of the chains in the crystal structure of **2**.

Based on the crystallographic data powder pattern were calculated for compound **1** and **2** and were compared with those measured, which proves that both compounds were obtained as pure phases (Figure S6 and S7 in the Supplemental). Scanning electron microscopy shows that for **2** crystalline particles of several μm were obtained (Figure S8 in the Supplemental).

Magnetic investigations

DC study

2

As already mentioned in the introduction, the main topic of this work focus on single chain magnetism and therefore, especially the chain compound **2** is of interest. However, for completeness we also measured the magnetic susceptibility of the discrete complex **1** as a function of temperature T in the temperature range 2 – 300 K. The χT vs. T dependence for **1** is shown in Figure S9. The value of χT monotonically decreases with decreasing temperature starting from 3.16 K·emu/mol at 290 K and ending at 1.77 K·emu/mol at 2.0 K. This behavior is well described by the simultaneous action of the spin-orbit coupling and the axial crystal field. The fit and fit parameters are given in Figure S9.

For the chain compound **2** the magnetic susceptibility was measured in the temperature range 2 – 300 K. The $\chi(T)$ dependence is presented in Figure 4. It has a sharp maximum at 3.9 K characteristic for an antiferromagnetic transition. In the inset the temperature dependence of the χT product is shown. The room temperature value of χT equals 3.3 emu·K/mol and is much greater than the spin only value 1.87, expected for s = 3/2, pointing to the orbital contribution in Co(II) which is also responsible for a small decrease of χT with decreasing temperature (not seen in the scale of the figure). However, below about 20 K a strong increase of χT is observed due to ferromagnetic intrachain interactions. Thus, the above mentioned antiferromagnetic transition can only be caused by weak antiferromagnetic interchain interactions.
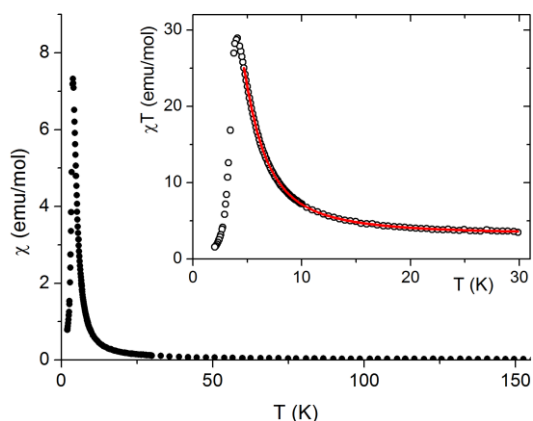

Figure 4. Temperature dependence of magnetic susceptibility χ and the χT product (inset) measured for **2** at 50 Oe. Solid line is a fit; see text.

For quasi one-dimensional anisotropic magnetic systems the temperature dependence of χT is often presented in the form of ln χT vs. reciprocal temperature plot (Figure S10 in the Supplemental). The slope of the linear part of this plot Δ_ξ/k_B = 11.9 K equals the energy for the creation of a domain wall and is a measure of the intrachain exchange interaction J. The value of J may be estimated from the relation $\Delta_\xi = 2s^2 J$,[27] thus, assuming s = 1/2 one obtains J/k_B ~23.8 K. The rounding down near the maximum may indicate antiferromagnetic interchain interactions. This behavior may be well described by the Ising hamiltonian adequate for linear chain of Co(II) ions in an axially distorted octahedral coordination

$$\mathcal{H} = -J \sum_i s_i^z s_{i+1}^z + \mu_B \sum_i H \cdot \hat{g} \cdot s_i, \qquad (1)$$

where the effective spin 1/2 is assumed at low temperatures in agreement with the Kramers doublet ground state of Co(II). The expression for susceptibility derived for $H \sim 0$ has the form[63]

$$\chi_\parallel^{chain} = \frac{N_A \mu_B^2 g_\parallel^2}{4 k_B T} \exp\left(\frac{J}{2 k_B T}\right), \qquad (2)$$

where $g_\parallel$ is the g-factor for H parallel to the easy axis of anisotropy. The perpendicular component of susceptibility

$\chi_\perp^{chain}$ is negligible at low temperatures. The interchain interaction zJ' may be accounted for in the mean field approximation

$$\chi_\parallel = \frac{\chi_\parallel^{chain}}{1 - zJ' \chi_\parallel^{chain}/(N_A g_\parallel^2 \mu_B^2)}, \qquad (3)$$

and susceptibility averaged for a powder sample calculated as

$$\chi = \chi_\parallel/3 + \chi_{tip}. \qquad (4)$$

The term χ_{tip} takes into account the increasing population of excited Kramers doublets of single Co(II) centers at elevated temperatures. Fitting such model to experimental data in the 5-30 K temperature range leads to the following values: J = 29.8(2) K, zJ' = –0.43(2) K, $g_\parallel$ = 7.2(1) and χ_{tip} = 0.034(1) emu/mol (Figure 4).

Such small interchain interaction zJ' may be easily overcome by magnetic field. To show this effect, the temperature dependent magnetic susceptibility was measured in various magnetic fields. The data obtained prove that a metamagnetic transition occurs between 200 and 400 Oe (Figure 5). It is noted that the fields given in the figure refer to the external fields and therefore, at 300 Oe an antiferromagnetic–like maximum is still visible especially, considering the fact that the sample is powdered and not all crystallites undergo metamagnetic transition at the same field.[64]
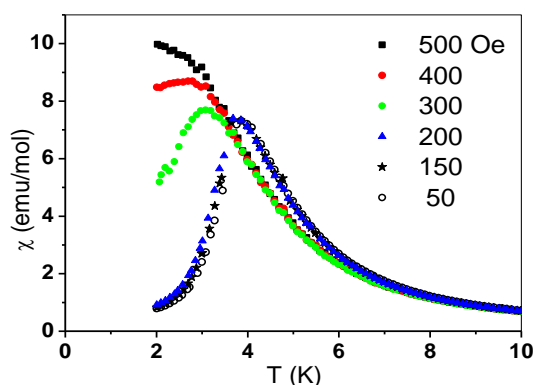
Figure 5. Magnetic susceptibility vs. temperature registered in various magnetic fields.

This transition is also clearly visible in field dependent magnetization measured at 2.0 K (Figure 6). The rapid increase of M below 2 kOe is followed by a slower increase up to 2.4 μ_B at 90 kOe. There is no saturation, seemingly because of the high anisotropy of Co(II) ions. No hysteresis loop is observed. The inset in Figure 6 shows $M(H)$ in the vicinity of the metamagnetic transition. The critical field H_c = 258±5 Oe at 2.0 K was determined from crossing of tangents to $M(H)$ curve below and above the transition. The values for H_c at higher temperatures were determined in the same way and used for the construction of the magnetic phase diagram (Figure 7). The additional points at higher temperatures were taken from the DC measurements at different fields (Figure 5).

Figure 6. Magnetization vs. field measured at $T = 2.0$ K for **2**. The inset magnifies the low-field region and shows the way of critical field determination.

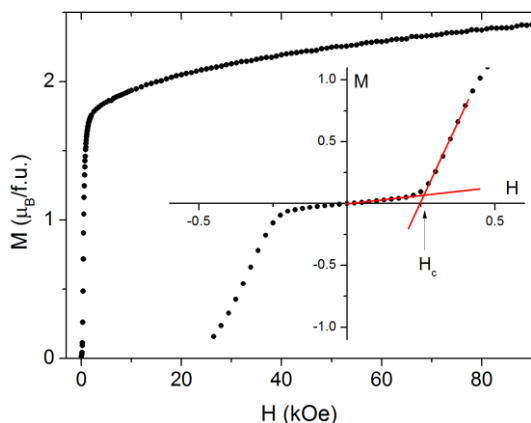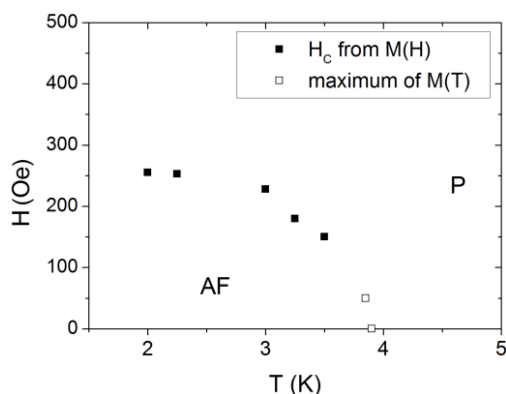**Figure 7.** Magnetic phase diagram of **2**.

performed under the field cooling (FC) and zero-field cooling (ZFC) regimes. Only small bifurcation between FC and ZFC curves in the limits of experimental uncertainties was observed, which does not clearly prove the presence of long time magnetic relaxations (Figure S11 in the Supplemental).

AC study

Figure 8 presents the temperature dependent AC magnetic susceptibility measured with the AC field amplitude of 5 Oe for various frequencies in a small DC field of 5 Oe. The measurements in higher DC fields: an intermediate field 360 Oe just above H_c and 1000 Oe far above H_c were also done for comparison. At 5 Oe a maximum at 3.89 K is observed in the χ' curve, that does not depend on frequency and originates from the antiferromagnetic phase transition. At lower temperatures the frequency dispersion appears in the antiferromagnetic state. However, χ'' component is observed in the wider temperature range up to 4.5 K. The χ'' maxima depend on frequency and show a temperature shift of their T_m positions. The Mydosh parameter φ determined according to equation

$$\varphi = \Delta T_m / [T_m \Delta(\log f)]. \tag{5}$$

is equal to 0.14, which is in the range expected for superparamagnets or single chain magnets. Above the critical field strong relaxations are observed. The $\chi'(T)$ maxima change their character and are not more a sign of the antiferromagnetic transition. This behavior is characteristic for the mixed phase in which 3D ferromagnetic domains appear.[64-66] Therefore, it cannot be described by a single relaxation process. In a still higher field the mixed phase fades and the chains are nearly decoupled. Because the object of our interest are single chain magnets, in the following we focus only on the relaxation behavior that is observed in fields below H_c.

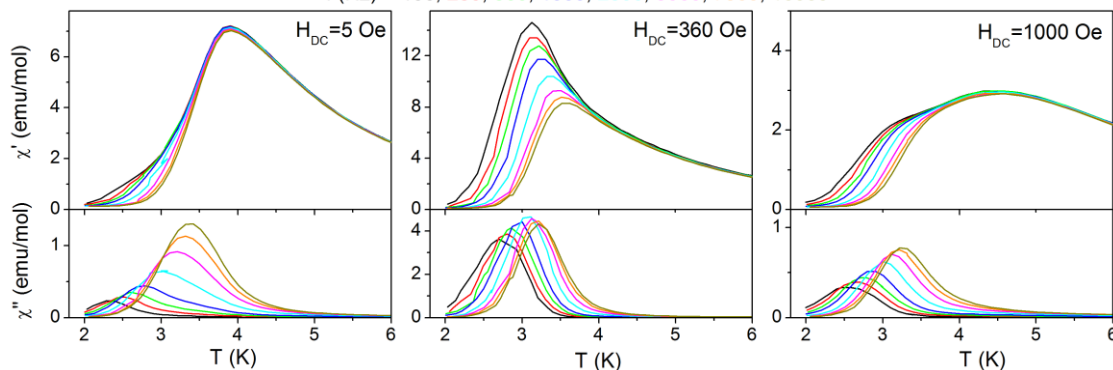Additional temperature dependent DC measurements, were

Figure 8. Temperature dependent AC magnetic susceptibilities for **2** measured for various frequencies in different DC magnetic fields.

In Figure 9 frequency dependent AC susceptibility measured at various temperatures in DC field of 5 Oe is presented. All frequency dependencies can be well described by the generalized Debye model with one mean relaxation time according to the equation

$$\chi = \chi' - i\chi'' = \chi_\infty + \frac{\chi_0 - \chi_\infty}{1 + (i2\pi f \tau)^{1-\alpha}} , \tag{6}$$

where χ_0 and χ_∞ are AC susceptibilities in the limit of zero and infinite frequency, respectively, τ is the mean relaxation time, f is the frequency of the AC field, α is a parameter related with the width of the relaxation times distribution ($0 \leq \alpha \leq 1$; $\alpha = 0$ means a unique relaxation time, $\alpha = 1$ means an infinity of relaxations times).

The table with the best fit parameters is given in the Supporting Information (Table S3). As seen in the Table, τ strongly

increases with decreasing temperature. The simultaneous increase of α means that the width of relaxation time distribution increases with decreasing temperature, which should be caused by interchain interactions. The Cole-Cole plots, which present χ'' vs. χ' dependence are shown in Figure 10. They are arc of circles which are shifted down with respect to the χ' axis according to the non-zero α parameter.
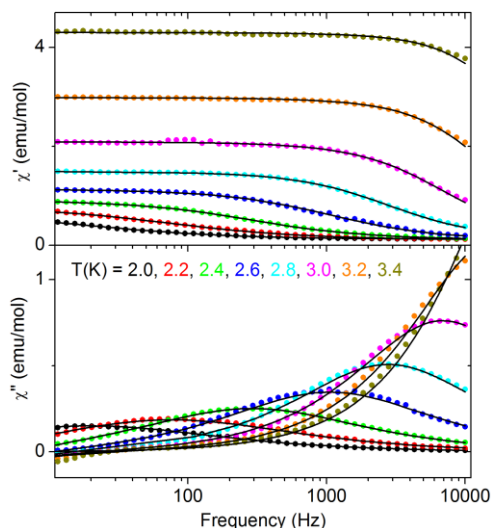
Figure 9. Frequency dependent AC susceptibility for **2** measured at various temperatures. Solid lines are fits with the generalized Debye model.
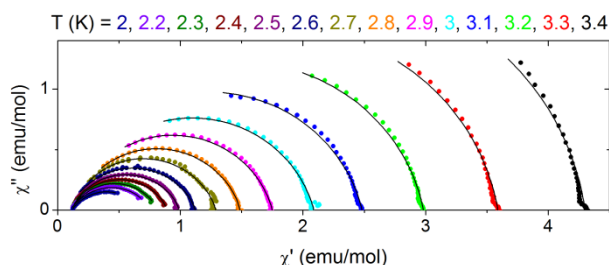

Figure 10. Cole-Cole plots for **2** at various temperatures. Solid lines are fits with the generalized Debye model.

The temperature dependence of τ is shown in Figure 11 as a plot of $\ln \tau$ *vs.* $1/T$, from which the energy barrier ΔE and prefactor τ_0 in the Arrhenius equation

$$\tau = \tau_0 \exp(\Delta E/k_B T) \qquad (7)$$

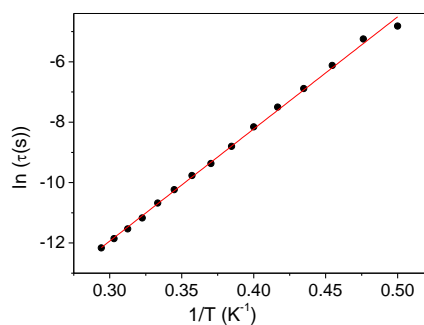can be determined. Their values are: $\Delta E/k_B = 37.1\pm0.5$ K and $\tau_0 = (9.5\pm1.0)\cdot10^{-11}$ s.

Figure 11. Logarithm τ vs. reciprocal temperature for **2**. Solid line is a linear fit.

Discussion of the magnetic properties

Compound **2,** built from ferromagnetic Co-(NCS)$_2$-Co chains, shows an antiferromagnetic transition at a Néel temperature of 3.8 K. It undergoes a metamagnetic transition in field of ~260 Oe. The magnetic relaxations existing in the antiferromagnetic state are well described with one mean relaxation time and single energy barrier for thermal activation $\Delta E/k_B = 37.1$ K, which may originate from single chain relaxations[67]

According to Coulon *et al.*[27] the activation energy of the relaxation time may be discussed using the following equation

$$\Delta E = k\Delta_\xi + \Delta_A , \qquad (8)$$

where Δ_ξ is the creation energy of the domain wall (here equal to $J/2$), k is a factor equal to 1 or 2, depending on whether we are dealing with finite or infinite chains, respectively, and Δ_A is the activation energy of a single uncoupled anisotropic spin. Assuming $k = 1$, a Δ_A value of 22.6 K is obtained for compound **2**. Thus the Glauber criterion $\Delta_A > \Delta_\xi$ is satisfied for Co(NCS)$_2$(ClBP)$_2$ chains in accordance with their Ising nature.

A crossover from $k = 1$ to $k = 2$ is expected with increasing temperature around T^*, that can be related to the chain length n[27]

$$2n\exp(-2Js^2/k_B T^*)\square = 1. \qquad (9)$$

However no change of slope (change of ΔE) is visible in Figure 11. If $k = 1$ and all points in the figure are below T^*, $1/T^* < 0.29$ K^{-1}, then $n < 50$ Co atoms for our sample of **2**. It is an acceptable limit.

As mentioned in the introduction compound **2** is a member of a family of compounds we have investigated in the past. All of these compounds of the general composition [Co(NCS)$_2$(L$_2$)]$_n$ (L = co-ligand) consist of octahedrally coordinated Co(II) cations that are linked into chains by pairs of thiocyanato anions. When the magnetic properties of these compounds are compared always similar values for the intrachain interaction are noted, which can be traced back to the fact that always the same thiocyanato chains are involved (Table 2). It is not clear if the small differences between the J values originate from the influence of the co-ligand.

Table 1: Selected magnetic parameters for compound **2** and related 1D compounds of composition [Co(NCS)$_2$(L)$_2$]$_n$ with (L = 4-Ethylpyridine (Etpy), 4-acetylpyridine (Acpy), 4-(3-phenylpropyl)pyridine (PPP), 1,2-bis(4-pyridiyl)-ethylene (bpe) and 1,2-bis(4-pyridiyl)-ethane (bpa). The parameters zJ' and J given below differ slightly from the values given in ref.[59-62] This is due to different models used to fit $\chi T(T)$ in some of these reports, particularly different definitions of zJ' and the temperature range used in the fitting procedures. To be able to compare directly between zJ' parameters for all compounds of this family, we estimated the parameters zJ' and J again, fitting $\chi T(T)$ data, but using the identical model as for **2**. For better comparison the value if Δ_A for the compound with Etpy was recalculated assuming $k=1$. Thus, it deviates from that given in ref.[60] where arbitrarily $k=2$ was selected. J = intrachain interaction; zJ' = interchain interaction; T_c = critical temperature; AF = antiferromagnetic ground state; FO = ferromagnetic ground state; H_c = critical field; ΔE = Arrhenius law energy; τ_0 = prefactor; Δ_A = see equation 8; α = distribution of the relaxation times determined at different temperatures; φ = Mydosh parameter.

5

	2	Etpy	bpe	bpa	Acpy	PPP
ground state	AF	AF	AF	AF	FM	FM
H_c (Oe)	~260 (2 K)	~175 (1.5 K)	~400 (2 K)	~40 (2K)	-	-
T_c (K)	3.9	3.4	4.0	3.1	3.8	3.3
J/k_B (K)	29.8	27.0	26.8	27.8	30.2	28.4
zJ'/k_B (K)	−0.43	−0.42	−0.66	−0.22	+0.17	+0.15
$\Delta E/k_B$ (K)	37.1	45.3	33.3	39.2	74	116
τ_0 (s)	9.5×10^{-11}	2×10^{-12}	1.2×10^{-11}	1.2×10^{-11}	6×10^{-13}	10^{-19}
Δ_A/k_B (K)	22.2 (k=1)	31.8 (k=1)	19.9 (k=1)	25.3 (k=1)	-	-
α	0.09 - 0.37	0.1 - 0.4	0.10 - 0.46	0.06 - 0.41	0.4 - 0.52	-
φ	0.14	0.14	0.16	0.11	0.074	0.059

However, all of these compounds can be divided into two different groups. The first group consists of compounds that exhibit an antiferromagnetic ground state and show a metamagnetic transition as it is the case for compound **2**. For all of these compounds the Mydosh parameter points to superparamagnetic behaviour, the magnetic relaxations can be well fitted using the Debye model leading to similar values for the anisotropy energy Δ_A and the Glauber criterion is also fulfilled. In this context it is noted that Δ_A can be also calculated in a more general way, without assuming the Fisher model restrictions, by using the Δ_ξ values obtained from the ln(chi$T$)(1/T) dependence. The values of Δ_A obtained in such a way do not differ very much from those given in table 2. Therefore, their relaxations seem to originate from the relaxation of single chains. However, for α, which is a measure for the distribution of the relaxation times, relatively large values are observed (Table 1). Even if such high values are frequently discussed in literature in context of single chain magnetic behaviour the question raises if this might always be adequate. With decreasing temperatures α increases dramatically which suggests that at higher temperatures single chain relaxations are observed, whereas at lower temperatures interchain interactions must come into play.

The second group consists of compounds with a ferromagnetic ground state. For these two compounds with 4-(3-phenylpropyl)pyridine (PPP) and 4-acetylpyridine (Acpy) as co-ligand a relatively small Mydosh parameter is observed indicating for spin glass-like behaviour (Table 2). Interestingly, for the Acpy compound the frequency dependent AC data can be fitted using the Debye model but in this case relatively high values of α and $\Delta E/k_B$ are obtained together with much smaller τ_0 value, which clearly shows that this compound behaves differently to that with the AF ground state. Moreover, temperature dependent AC data obtained for the compound with PPP lead to an unrealistic small τ_0, so obtained ΔE cannot be linked with the relaxation process of single chains. All these findings indicate that for the ferromagnetic compounds the relaxation might not be traced back to the relaxation of single chains and that it is more reasonable to assume that these are relaxations of walls of 3-dimensional ferromagnetic domains.

The reason why some of these compounds exhibits an antiferromagnetic whereas some others exhibits a ferromagnetic ground state is still unclear. There is, e.g., no simple correlation between the interchain distances and their magnetic properties. It is noted that two different arrangements of the Co(NCS)$_2$ chains are observed in their crystal structures. In some of these compounds the N-N vector of the two coordinating pyridine ligands of neighboring chains are parallel, whereas in some others they are canted. Unfortunately this does not correlate with the magnetic ground state of these compounds. Most probably, the type of the magnetic ground state is due to different arrangements of the anisotropic Co chains in the crystal

structures, which lead to different dipolar interactions changing the sign of effective zJ'. The basis for the simulations of dipolar interactions and expected ground state is however single ion Co anisotropy and its direction, which is not obvious. To gain such information magnetic investigations with a single crystal would be desirable.

Conclusions

In the present contribution a new thiocyanato compound with the relatively large co-ligand 4-(4-chlorobenzyl)pyridine was prepared, in which the Co(II) cations are linked by pairs of thiocyanato anions into chains. This new compound is a member of a family of compounds that we have recently investigated to examine the influence of a chemical and a structural modification onto the magnetic properties in detail. For some of these compounds the magnetic properties can be discussed as single chain magnetic behavior, while for some other compounds this seems to be inadequate. Within this family, compound **2** presented in this report, in spite of undergoing an antiferromagnetic transition, most clearly demonstrates the relaxation behavior characteristic for single chain magnets.

In this context it is noted that the stem compound Co(NCS)$_2$(pyridine) mentioned in the introduction obviously also exhibits a ferromagnetic ground state but shows relaxations which were interpreted as SCM relaxations on the basis of the Mydosh parameter, α and the analysis of the relaxation times.[54] In this work these parameters were determined by a different procedure and the temperature dependence of α was not investigated and therefore, these results cannot be compared here. However, in the light of the results of this work the question araises how this compound can be classified and what the real nature of its relaxations is. Consequently, these questions must be answered in future investigations.

Experimental Section

Co(NCS)$_2$ and 4-(4-chlorobenzyl)pyridine (ClBP) were obtained from Alfa Aesar. Solvents were used without further purification. The crystalline powders of all compounds were prepared by stirring the reactants in the respective solvents at room temperature. The purity of the compounds was checked by X-ray powder diffraction and elemental analysis.

*Synthesis of Co(NCS)$_2$(4-(4-chlorobenzyl)pyridine)$_4$ (**1**):*

Single crystals suitable for single crystal X-ray diffraction were prepared by Co(NCS)$_2$ (26.3 mg, 0.15 mmol) 4-(4-chlorobenzyl)pyridine (105.4 μL, 0.60 mmol) in 1.5 mL acetonitrile. A crystalline powder was synthesized by stirring Co(NCS)$_2$ (175.1 mg, 1.00 mmol) and 4-(4-chlorobenzyl)pyridine (702.3 μL, 4.00 mmol) in 5 mL acetonitril for 6 d. Yield: 85 % elemental analysis calcd (%) for

6

$C_{50}H_{40}Cl_4CoN_6S_2$: C 60.67, H 4.07, N 8.49; S 6.48; found C 59.33, H 4.24, N 8.31, S 6.89. IR (ATR): ν_{max} = 3075 (w), 3039 (w),2915 (w), 2064 (s), 2084 (s), 1615 (s), 1558 (m), 1488 (s), 1422 (s), 1348 (w), 1311 (w), 1222 (m), 1091 (m), 1048 (m), 1014 (s), 923 (w), 855 (s), 805 (s), 799 (s), 733 (m), 714 (m), 675 (w), 592 (s), 490 (s), 423 (m).

Synthesis of [Co(NCS)₂(4-(4-chlorobenzyl)pyridine)₂]ₙ (2):
Single crystals suitable for single crystal X-ray diffraction were prepared by Co(NCS)₂ (52.5 mg, 0.30 mmol) 4-(4-chlorobenzyl)pyridine (26.4 µL, 0.15 mmol) in 1.5 mL methanol. A crystalline powder was synthesized by stirring Co(NCS)₂ (175.1 mg, 1.00 mmol) and 4-(4-chlorobenzyl)pyridine (93.8 µL, 0.50 mmol) in 5 mL water for 3 d. Yield: 77 % elemental analysis calcd (%) for $C_{26}H_{20}Cl_2CoN_4S_2$: C 53.62, H 3.46, N 9.62; S 11.01; found C 53.36, H 3.35, N 9.40, S 10.86. IR (ATR): ν_{max} = 3086 (w), 3027 (w),2905 (w), 2105 (s), 2084 (s), 1692 (w), 1612 (s), 1558 (m), 1488 (s), 1423 (s), 1274 (w), 1223 (m), 1094 (m), 1068 (m), 1014 (s), 919 (w), 852 (m), 805 (s), 787 (s), 733 (m), 656 (w), 597 (s), 503 (s), 489 (s), 423 (m).

Elemental Analysis
CHNS analysis was performed using an EURO EA elemental analyzer fabricated by EURO VECTOR Instruments and Software.

IR-Spectroscopy
All IR data were obtained using an ATI Mattson Genesis Series FTIR Spectrometer, control software: WINFIRST, from ATI Mattson.

Differential Thermal Analysis and Thermogravimetry (DTA-TG)
The DTA-TG measurements were performed in a nitrogen atmosphere (purity: 5.0) in Al_2O_3 crucibles using a STA-409CD instrument from Netzsch. All measurements were performed with a flow rate of 75 mL·min⁻¹ and were corrected for buoyancy and current effects. The instrument was calibrated using standard reference materials.

Scanning electronmicroscopy (SEM)
The SEM measurements were performed with a Philips Environmental Scanning Electron Microscope ESEM XL30, which is equipped with an EDAX detector.

Magnetic measurements
Magnetic measurements were performed using a PPMS (Physical Property Measurement System) from Quantum Design. All AC data were obtained with the amplitude of the AC field equal to 5 Oe. The data were corrected for core diamagnetism.

X-Ray Powder Diffraction (XRPD)
The measurements were performed using 1) a PANalytical X'Pert Pro MPD Reflection Powder Diffraction System with CuKα radiation (λ = 154.0598 pm) equipped with a PIXcel semiconductor detector from PANanlytical and 2) a Stoe Transmission Powder Diffraction System (STADI P) with CuKα radiation (λ = 154.0598 pm) that was equipped with a linear position-sensitive detector from STOE & CIE.

Single Crystal Structure analysis
The data collection was performed with imaging plate diffraction systems (STOE IPDS-1 (**1**), STOE IPDS-2 (**2**)) using MoKα radiation. The structure solution was done with direct methods using SHELXS-97 and structure refinement was performed against F2 using SHELXL-97.[68] For both compounds a numerical absorption correction was applied using X-red and X-shape of the Program Package X-area.[69-71] All non-hydrogen atoms were refined with anisotropic displacement parameters.

All hydrogen atoms were positioned with idealized geometry and were refined isotropically with $U_{iso}(H) = -1.2\ U_{eq}(C)$ (1.5 for methyl H). Selected crystal data and details of the structure determinations are given in Table .

Table 2: Selected crystal data and details on the structure determination of compounds **1** and **2**.

Compound	1	2
formula	$C_{50}H_{40}Cl_4CoN_6S_2$	$C_{26}H_{20}Cl_2CoN_4S_2$
MW / g mol⁻¹	989.73	582.41
crystal system	*monoclinic*	*triclinic*
space group	*C*2/c	*P*-1
Z	4	2
D_{calc} / mg cm⁻³	1.382	1.482
μ / mm⁻¹	0.715	1.045
a / Å	18.8098(13)	9.0456(15)
b / Å	9.5685(5)	10.8405(16)
c / Å	27.6126(17)	14.941(3)
α / °	90	73.393(19)
β / °	106.867(7)	83.37(2)
γ / °	90	68.356(17)
V / Å³	4756.0(5)	1304.9(4)
T / K	293(2)	200(2)
scan range 2θ / deg	2.26 to 25.97	2.10 to 26.99
measured refl.	20774	18952
R_{int}	0.0389	0.0413
min/max. transm.	0.7998, 0.8759	0.7951, 0.9070
unique reflns.	4584	5692
refl.[F₀>4σ(F₀)]	3894	4342
parameters	296	320
R_1 [F₀ > 4σ(F₀)]	0.0357	0.0441
wR_2 [all data]	0.0946	0.1021
GOF	1.057	1.034
$\Delta\rho_{max/min}$/e Å⁻³	0.428 and -0.394	0.380 and -0.437

Notes
ᵃ Institut für Anorganische Chemie, Christian-Albrechts-Universität zu Kiel, Max-Eyth-Straße 2, 24118 Kiel, Germany. Fax: +49 431-880 1520; Tel: +49 431-880 1520; E-mail: cnaether@ac.uni-kiel.de

ᵇInstitute of Physics, Jagiellonian University, 30-348 Kraków, Łojasiewicza 11, Poland.

cMartin-Luther-Universität Halle-Wittenberg, Institut für Chemie, Kurt-Mothes-Straße 2, 06120 Halle / Saale, Germany.

ReferencesUncategorized References

[1] W. L. Leong, J. J. Vittal, *Chem. Rev.* **2011**, *111*, 688-764.

[2] H. Arora, F. Lloret, R. Mukherjee, *Inorg. Chem.* **2009**, *48*, 1158-1167.

[3] L. Bogani, C. Sangregorio, R. Sessoli, D. Gatteschi, *Angew. Chem.* **2005**, *117*, 5967-5971.

[4] S. W. Choi, H. Y. Kwak, J. H. Yoon, H. C. Kim, E. K. Koh, C. S. Hong, *Inorg. Chem.* **2008**, *47*, 10214-10216.

[5] E. Shurdha, C. E. Moore, A. L. Rheingold, S. H. Lapidus, P. W. Stephens, A. M. Arif, J. S. Miller, *Inorg. Chem.* **2013**, *52*, 10583-10594.

[6] X. Shen, Q. Zhang, H. Zhou, H. Zhou, A. Yuan, *New J. Chem.* **2012**, *36*, 1180-1186.

[7] P. P. Chakrabarty, S. Saha, D. Schollmeyer, A. K. Boudalis, A. D. Jana, D. Luneau, *J. Coord. Chem.* **2012**, *66*, 9-17.

[8] C. Näther, S. Wöhlert, J. Boeckmann, M. Wriedt, I. Jeß, *Z. Anorg. Allg. Chem.* **2013**, *639*, 2696-2714.

[9] M. Bałanda, Z. Tomkowicz, W. Haase, M. Rams, *J. Phys.: Conf. Ser.* **2010**, *303*, 012036.

[10] A. Caneschi, D. Gatteschi, N. Lalioti, C. Sangregorio, R. Sessoli, G. Venturi, A. Vindigni, A. Rettori, M. G. Pini, M. A. Novak, *Angew. Chem.* **2001**, *113*, 1810-1813.

[11] E. Pardo, R. Ruiz-García, F. Lloret, J. Faus, M. Julve, Y. Journaux, M. Novak, F. Delgado, C. Ruiz-Pérez, *Chem. Eur. J.* **2007**, *13*, 2054-2066.

[12] H.-L. Sun, Z.-M. Wang, S. Gao, *Coord. Chem. Rev.* **2010**, *254*, 1081-1100.

[13] L. Bogani, A. Vindigni, R. Sessoli, D. Gatteschi, *J. Mater. Chem* **2008**, *18*, 4733–4880.

[14] W.-X. Zhang, R. Ishikawa, B. Breedlovea, M. Yamashita, *RSC Adv.* **2013**, *3*, 3772-3798.

[15] J. Ru, F. Gao, T. Wu, M.-X. Yao, Y.-Z. Li, J.-L. Zuo, *Dalton Trans.* **2014**, *43*, 933-936.

[16] E. V. Peresypkina, A. M. Majcher, M. Rams, K. E. Vostrikova, *Chem. Commun.* **2014**, *50*, 7150-7153.

[17] H. Miyasaka, R. Clérac, *Bull. Chem. Soc. Jpn.* **2005**, *78*, 1725-1748.

[18] A. V. Palii, O. S. Reu, S. M. Ostrovsky, S. I. Klokishner, B. S. Tsukerblat, Z.-M. Sun, J.-G. Mao, A. V. Prosvirin, H.-H. Zhao, K. R. Dunbar, *J. Am. Chem. Soc.* **2008**, *130*, 14729-14738.

[19] M. Bałanda, M. Rams, S. K. Nayak, Z. Tomkowicz, W. Haase, K. Tomala, J. V. Yakhmi, *Phys. Rev. B* **2006**, *74*, 224421.

[20] Z. Tomkowicz, M. Rams, M. Bałanda, S. Foro, H. Nojiri, Y. Krupskaya, V. Kataev, B. Büchner, S. K. Nayak, J. V. Yakhmi, W. Haase, *Inorg. Chem.* **2012**, *51*, 9983-9994.

[21] S.-Y. Zhang, W. Shi, Y. Lan, N. Xu, X.-Q. Zhao, A. K. Powell, B. Zhao, P. Cheng, D.-Z. Liao, S.-P. Yan, *Chem. Commun.* **2011**, *47*, 2859-2861.

[22] X. Feng, T. David Harris, J. R. Long, *Chem. Sci.* **2011**, *2*, 1688-1694.

[23] R. Liu, L. Li, X. Wang, P. Yang, C. Wang, D. Liao, J.-P. Sutter, *Chem. Commun.* **2010**, *46*, 2566-2568.

[24] V. Mougel, L. Chatelain, J. Hermle, R. Caciuffo, E. Colineau, F. Tuna, N. Magnani, A. de Geyer, J. Pécaut, M. Mazzanti, *Angew. Chem.* **2014**, *126*, 838-842.

[25] Y.-L. Hou, R.-R. Cheng, G. Xiong, J.-Z. Cui, B. Zhao, *Dalton Trans.* **2014**, *43*, 1814-1820.

[26] H. Miyasaka, T. Madanbashi, A. Saitoh, N. Motokawa, R. Ishikawa, M. Yamashita, S. Bahr, W. Wernsdorfer, R. Clérac, *Chem. – Eur. J.* **2012**, *18*, 3942-3954.

[27] C. Coulon, H. Miyasaka, R. Clérac, *Struct. Bond.* **2006**, *122*, 163-206.

[28] J. H. Yoon, J. W. Lee, D. W. Ryu, S. W. Yoon, B. J. Suh, H. C. Kim, C. S. Hong, *Chem. Eur. J.* **2011**, *17*, 3028-3034.

[29] J. H. Yoon, W. R. Lee, D. W. Ryu, J. W. Lee, S. W. Yoon, B. J. Suh, H. C. Kim, C. S. Hong, *Inorg. Chem.* **2011**, *50*, 10777-10785.

[30] X.-B. Li, G.-M. Zhuang, X. Wang, K. Wang, E.-Q. Gao, *Chem. Commun.* **2013**, *49*, 1814-1816.

[31] A. Escuer, G. Vlahopoulou, F. A. Mautner, *Inorg. Chem.* **2011**, *50*, 2717-2719.

[32] F. A. Mautner, M. Scherzer, C. Berger, R. C. Fischer, R. Vicente, S. S. Massoud, *Polyhedron* **2015**, *85*, 20-26.

[33] B. Machura, A. Świtlicka, P. Zwoliński, J. Mroziński, B. Kalińska, R. Kruszynski, *J. Solid State Chem.* **2013**, *197*, 218-227.

[34] B. Machura, A. Świtlicka, J. Mroziński, B. Kalińska, R. Kruszynski, *Polyhedron* **2013**, *52*, 1276-1286.

[35] J. G. Małecki, T. Groń, H. Duda, *Polyhedron* **2012**, *36*, 56-68.

[36] Q. Ma, M. Zhu, L. Lu, S. Feng, J. Yan, *Inorg. Chim. Acta* **2011**, *370*, 102-107.

[37] M. Wriedt, C. Näther, *Chem. Commun.* **2010**, *46*, 4707-4709.

[38] J. Boeckmann, C. Näther, *Polyhedron* **2012**, *31*, 587-595.

[39] S. Wöhlert, J. Boeckmann, M. Wriedt, C. Näther, *Angew. Chem., Int. Ed.* **2011**, *50*, 6920–6923.

[40] P. Bhowmik, S. Chattopadhyay, M. G. B. Drew, C. Diaz, A. Ghosh, *Polyhedron* **2010**, *29*, 2637-2642.

[41] S. Wöhlert, U. Ruschewitz, C. Näther, *Cryst. Growth Des.* **2012**, *12*, 2715-2718.

[42] S. Wöhlert, J. Boeckmann, I. Jess, C. Näther, *CrystEngComm* **2012**, *14*, 5412-5420.

[43] S. Wöhlert, L. Peters, C. Näther, *Dalton Trans.* **2013**, *42*, 10746-10758.

[44] C. J. Adams, M. F. Haddow, D. J. Harding, T. J. Podesta, R. E. Waddington, *CrystEngComm* **2011**, *13*, 4909-4914.

[45] A. Barasiński, P. Sobczak, A. Drzewiński, G. Kamieniarz, A. Bieńko, J. Mroziński, D. Gatteschi, *Polyhedron* **2010**, *29*, 1485-1491.

[46] S. Wöhlert, T. Runčevski, R. E. Dinnebier, S. G. Ebbinghaus, C. Näther, *Cryst. Growth Des.* **2014**, *14*, 1902-1913.

[47] S. Wöhlert, M. Wriedt, T. Fic, Z. Tomkowicz, W. Haase, C. Näther, *Inorg. Chem.* **2013**, *52*, 1061-1068.

[48] J. G. Małecki, P. Zwoliński, *Polyhedron* **2012**, *39*, 85-90.

[49] J.-F. Létard, S. Asthana, H. J. Shepherd, P. Guionneau, A. E. Goeta, N. Suemura, R. Ishikawa, S. Kaizaki, *Chem. Eur. J.* **2012**, *18*, 5924-5934.

[50] S. Das, K. Bhar, S. Chattopadhyay, P. Mitra, V. J. Smith, L. J. Barbour, B. K. Ghosh, *Polyhedron* **2012**, *38*, 26-35.

[51] J. G. Małecki, B. Machura, A. Świtlicka, T. Groń, M. Bałanda, *Polyhedron* **2011**, *30*, 746-753.

[52] J. Palion-Gazda, B. Machura, F. Lloret, M. Julve, *Cryst. Growth Des.* **2015**, *15*, 2380-2388.

[53] R. González, A. Acosta, R. Chiozzone, C. Kremer, D. Armentano, G. De Munno, M. Julve, F. Lloret, J. Faus, *Inorg. Chem.* **2012**, *51*, 5737-5747.

[54] J. Boeckmann, C. Näther, *Dalton Trans.* **2010**, *39*, 11019-11026.

8

[55]   J. Boeckmann, C. Näther, *Chem. Commun.* **2011**, *47*, 7104-7106.

[56]   S. Foner, R. B. Frankel, W. M. Reiff, B. F. Little, G. J. Long, *Solid State Commun.* **1975**, *16*, 159-161.

[57]   S. Foner, R. B. Frankel, W.M. Reiff, H. Wong, G. J. Long, *J. Chem. Phys.* **1978**, *68*, 4781-4783.

[58]   J. Boeckmann, M. Wriedt, C. Näther, *Chem. Eur. J.* **2012**, *18*, 5284-5289.

[59]   M. R. Julia Werner, Zbigniew Tomkowicz, Tomče Runčevski, Robert E. Dinnebier, Stefan Suckert and Christian Näther, *Inorg. Chem.* **2015**, *54*, 2893.

[60]   S. Wöhlert, T. Fic, Z. Tomkowicz, S. G. Ebbinghaus, M. Rams, W. Haase, C. Näther, *Inorg. Chem.* **2013**, *52*, 12947-12957.

[61]   S. Wöhlert, Z. Tomkowicz, M. Rams, S. G. Ebbinghaus, L. Fink, M. U. Schmidt, C. Näther, *Inorg. Chem.* **2014**, *53*, 8298–8310.

[62]   J. Werner, M. Rams, Z. Tomkowicz, C. Nather, *Dalton Trans.* **2014**, *43*, 17333-17342.

[63]   M. E. Fisher, *J. Math. Phys.* **1963**, *4*, 124-135.

[64]   R. L. Carlin, A. J. van Duyneveldt, *Acc. Chem. Res.* **1980**, *13*, 231-236.

[65]   R. Hoogerbeets, S. A. J. Wiegers, A. J. van Duyneveldt, R. D. Willett, U. Geiser, *Physica B* **1984**, *125*, 135-149.

[66]   C. Coulon, R. Clérac, W. Wernsdorfer, T. Colin, H. Miyasaka, *Phys. Rev. Lett.* **2009**, *102*, 164204-164207.

[67]   H. Miyasaka, K. Takayama, A. Saitoh, S. Furukawa, M. Yamashita, R. Clérac, *Chem. Eur. J.* **2010**, *16*, 3656-3662.

[68]   G. M. Sheldrick, *Acta Cryst.* **2008**, *A64*, 112-122.

[69]   *X-Area, Version 1.44, Program Package for Single Crystal Measurements*, STOE & CIE GmbH, Darmstadt, Germany, **2008**.

[70]   *X-Red, Version 1.11, Program for Data Reduction and Absorption Correction*, STOE & CIE GmbH, Darmstadt, Germany, **1998**.

[71]   *X-Shape, Version 1.03, Program for the Crystal Optimization for Numerical Absorption Correction*, STOE & CIE GmbH, Darmstadt, Germany, **1998**.

Synthesis, Structure and Properties of [Co(NCS)$_2$(4-(4-Chlorobenzyl) pyridine)$_2$]$_n$, that shows Slow Magnetic Relaxations and a Metamagnetic Transition

Julia Werner, Zbigniew Tomkowicz, Michał Rams, Stefan G. Ebbinghaus, Tristan Neumann and Christian Näther
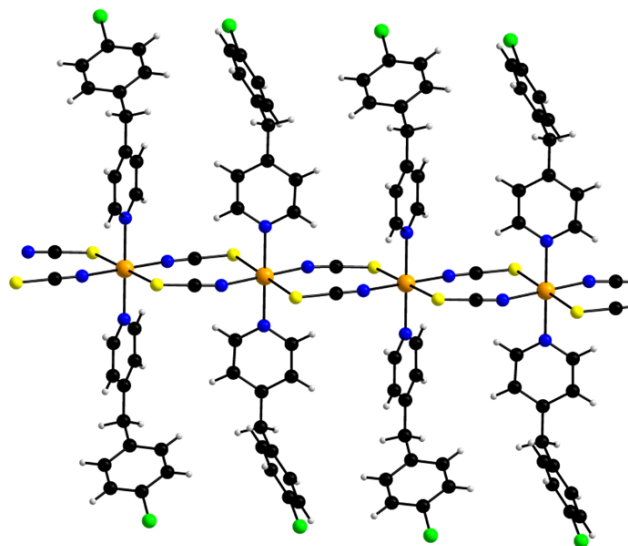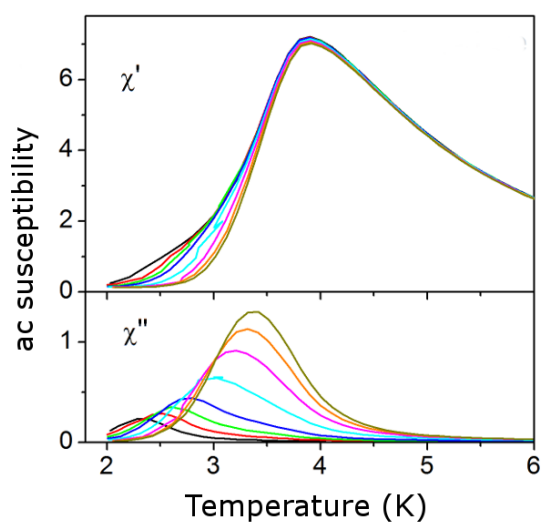
[Co(NCS)$_2$(4-(4-Chlorobenzyl)pyridine)$_2$]$_n$ shows metamagnetic behavior and slow relaxations of the magnetization indicative for single chain magnet behavior.